Time-resolved photoluminescence and optically stimulated luminescence measurements of picosecond-excited SrS:Ce,Sm phosphor

F. Ravotti, D. Benoit, P. Lefèbvre, P. Valvin, J.-R. Vaillé, L. Dusseau, J. Fesquet, J. Gasiot

Time-resolved photoluminescence and optically stimulated luminescence measurements of picosecond-excited SrS:Ce,Sm phosphor

F. Ravotti[a] and D. Benoit
Institut d'Electronique du Sud–UMR UMII-CNRS 5214, Université Montpellier II, Place E. Bataillon, CC 083, 34095 Montpellier Cedex 5, France

P. Lefebvre and P. Valvin
Groupe d'Etude des Semiconducteurs–UMR UMII-CNRS 5650, Université Montpellier II, Place E. Bataillon, CC 074, 34095 Montpellier Cedex 5, France

J.-R. Vaillé, L. Dusseau, J. Fesquet, and J. Gasiot
Institut d'Electronique du Sud–UMR UMII-CNRS 5214, Université Montpellier II, Place E. Bataillon, CC 083, 34095 Montpellier Cedex 5, France

(Received 22 August 2007; accepted 19 October 2007; published online 18 December 2007)

Doubly activated alkaline-earth phosphors are known to present luminescent and charge-storage properties. In this work, we investigate the photoluminescence (PL) and the optically stimulated luminescence (OSL) of the SrS:Ce,Sm phosphor by means of time-resolved spectroscopy with excitation laser pulses of 2 ps duration. By comparing the PL measurements obtained with direct UV excitation and the OSL experiments performed using infrared wavelength, it was possible to measure a charge conversion lifetime of about 2.5 ± 1 ns. A luminescence lifetime of 36 ± 1 ns has also been found. These measurements are presented and discussed in connection with applications where the speed of the SrS:Ce,Sm luminescence is a crucial parameter. © *2007 American Institute of Physics*. [DOI: 10.1063/1.2822474]

I. INTRODUCTION

Doubly activated alkaline-earth sulfides present interesting luminescent and charge-storage properties that have been known for a number of years. Activators are rare-earth elements, which have ground and excited states in the forbidden wide band gap of the sulfide host (3–6 eV). Upon exposure to ionizing radiation, photoluminescent emission in the visible wavelength range occurs due to electronic transitions involving one of the two dopants (properly called "activator"); however, some excited electrons are trapped by the other dopant ("coactivator") that is thought to be an electron trapping site. Releasing those trapped electrons requires energy that is provided by stimulating the material with infrared (IR) light. The so created free electrons can therefore recombine with the previously ionized activator, emitting visible photons ($\lambda = 400–700$ nm). This second mechanism, being promoted by the infrared light, is referred to as the optically stimulated luminescence (OSL).

Several sulfides (SrS, MgS, and CaS) activated with europium (Eu) or cerium (Ce) and coactivated by samarium (Sm) have been investigated in literature as OSL materials.[1–3] The choice of sulfides as host materials resides in their relatively simple synthesizing procedure. They are suitable for infrared detection, near-IR-to-visible converters,[4] and radiation dose measurement,[5] and they are expected to be developed as erasable and rewritable optical memories.[6,7]

The University Montpellier II in France, developed a sulfide optimized for radiation dosimetry.[8] The SrS:Ce,Sm synthesized in Montpellier is now used for dose mapping in medical applications[9] and for in-flight dosimetry in space applications,[10] and it has been recently proposed also for the radiation monitoring in high-energy physics (HEP) facilities.[11] For this last application, the possibility to build probes based on SrS:Ce,Sm crystals coupled to the extremity of optical fibers has been experimented on with success.[12]

Such fibered monitoring devices present the advantage of reduced dimensions, high radiation hardness, and immunity to the electronic noise since the photoluminescence (PL) and OSL signals, as well as the IR stimulation light, are transmitted by optical ways.

Apart from charge-storage properties, rare-earth activated alkaline-earth sulfides have short luminescence lifetimes and fast charge conversion that have been rarely explored in literature. The natural extension of the radiation monitoring with fibered SrS:Ce,Sm crystals in hostile radiation environments is therefore the simultaneous application in the detection of very high speed phenomena. Examples of those are the *pp* collisions at the interaction points of the ATLAS and CMS experiments of the CERN Large Hadron Collider (LHC).[13] There, the 7 TeV proton bunch interactions, spaced by 25 ns, generate a harsh radiation field of 10^{15} p/cm^2, composed mostly of pions, over ten years of operation. Radiation hard detectors able to monitor the crossing beams on a bunch-by-bunch basis are being developed to detect anomalous beam events that would cause a background to the normal events of colliding protons (for example, beam gas interactions) or, even more drastically, cause a danger to the detectors of the experiments themselves.

For detecting fast phenomena, the time response characteristics of the SrS:Ce,Sm needs to be evaluated in detail. For

[a]Also at CERN, 1211 Geneva 23, Switzerland. Electronic mail: Federico.Ravotti@cern.ch.

this purpose, time-resolved measurements at PL and OSL excitation wavelengths were performed. With this technique, a SrS:Ce,Sm sample is excited by a series of optical pulses that generate a repetition of emission/relaxation phases that are subsequently recorded by a streak camera.[14]

Similar studies have been reported in literature for SrS and CaS activated with Eu and Sm using excitation sources on the nanosecond[15] and picosecond[16] scales. In those experiments, the excitation light had a minimum pulse duration of 20 ps. Time-resolved PL and OSL experiments of SrS:Ce,Sm, excited by 2 ps laser pulses, are reported and discussed here. The results are analyzed by using the existing models for the SrS:Ce,Sm phosphor and discussed in connection with its potential applications where the luminescence lifetime has to be considered as a crucial parameter, namely, "bunch-by-bunch" particle detection in HEP and the readout speed in charge-storage applications.

II. MATERIAL AND EXPERIMENTAL DETAILS

The SrS host sulfide has been obtained following the procedure described elsewhere.[17] The final material presents concentrations in Ce and Sm on the order of 0.1 wt % and 0.05 wt %, respectively.[8] For time-resolved experiments, a SrS:Ce,Sm crystal of a few mm^2 has been selected according to the intensity of its UV-excited luminescence. This crystal was polished on one side in order to minimize the diffusion of the excition photons provided by the laser light.

The experiments have been carried out with a time-resolved spectroscopy setup consisting in a continuous-mode Ar^{++} laser, pumping a Al_2O_3:Ti cavity that delivers laser pulses with duration of 2 ps and fundamental frequency (ω_f) in the near IR. Before reaching the sample, nonlinear crystals were used to generate photons with increased frequency until the UV range, while a pulse picker allows the selection of the repetition rate of the laser pulses. For the experiments presented in this article, OSL measurements have been performed with $\lambda_f = 805$ nm with an energy of 5 nJ per pulse, while PL excitations were provided with photons at $3\omega_f$ (i.e., $\lambda = 260$ nm) and energy of about 5 pJ per pulse. The repetition rate has been set to 80 kHz, which corresponds to the delivery of one laser pulse every 12.5 μs. The choice of such a repetition period has been adapted to the luminescence phenomenon under observation.

The PL and OSL signals emitted at RT (21 °C) by the excited SrS:Ce,Sm crystal were analyzed by a spectrometer (focal length of 500 mm with 150 g/mm grating) and time resolved by means of a Hamamatsu C4334 streak camera. In order to suppress the photons diffused by the sample at the UV ($\lambda < 400$ nm) and IR ($\lambda > 700$ nm) excitation wavelengths, a series of complementary filters has been installed in front of the spectrometer slit. The streak camera was used, in our experiment, to produce images of the luminescent signal (640×480 pixels) over a spectroscopic window of 60 nm centered on a selectable wavelength (λ_c), for the horizontal scale, and with a minimum time sweep range of 50 ns, for the vertical scale.

For PL measurements, 2 ps UV-pulse trains are sent on the SrS:Ce,Sm, and the corresponding luminescence, emitted after each pulse, is integrated in order to obtain a proper statistics. The same approach has been used for the OSL measurements. In this case, the trapped charge has been first generated at RT by exposing the material for 5 min to a constant flux of UV light with 254 nm wavelength from a 6 W lamp. The 2 ps IR-pulse train was then started immediately after the UV exposure since no afterglow phenomena were observed in the SrS:Ce,Sm under test. The trapped electrons freed during stimulation generate an OSL signal that decreases with increasing stimulation time. The IR stimulation was therefore run until the material was completely depleted by the laser pulse train. In order to improve the signal-to-noise-ratio of the OSL, the above procedure has been repeated 20 times and the different OSL images have been averaged during data analysis.

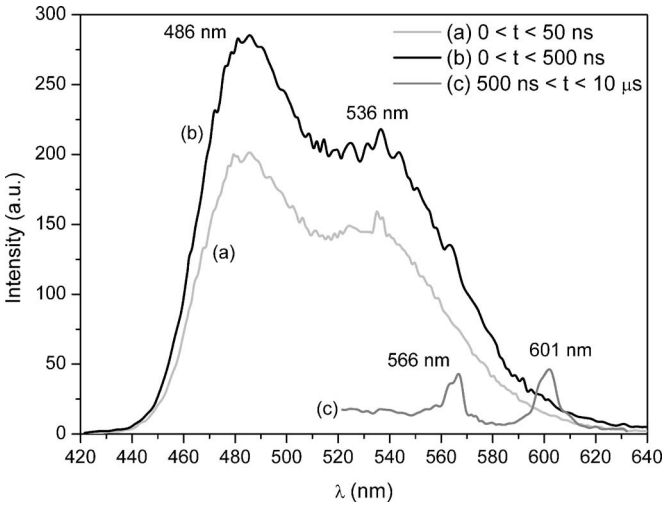

FIG. 1. Photoluminescent (PL) spectra from the SrS:Ce,Sm phosphor following a 260 nm excitation. The curves a, b, and c refer to different integration time windows over the streak camera images. The intensities of the different spectra (in arbitrary units) have not been normalized.

III. RESULTS

A. Spectral analysis

Figure 1 shows the time-resolved PL spectra measured upon laser excitation at 260 nm. The three curves (labeled a–c) refer to PL spectra integrated over different time intervals following the UV excitation. The a curve shows the fast-luminescent spectrum recorded in the first 50 ns after excitation, which presents an intense peak at 486 nm and a shoulder at 536 nm. This spectrum remains essentially unchanged, when the integration time is extended to 500 ns (curve b of Fig. 1). The PL spectrum recorded after 500 ns from the stimulation and integrated over a longer time range (until 10 μs) presents a completely different behavior, as shown in curve c of Fig. 1. Two new weak emission lines appear at 566 and 601 nm, while the previous fast spectrum is completely extinguished.

An update on the optical proprieties of the Montpellier's SrS:Ce,Sm phosphor has been recently published by Lapraz *et al.*[18] and reprinted here in Fig. 2. According to this work and other independent sources[19] investigating Ce-doped SrS phosphors, the intense fast emissions observed at 486 and

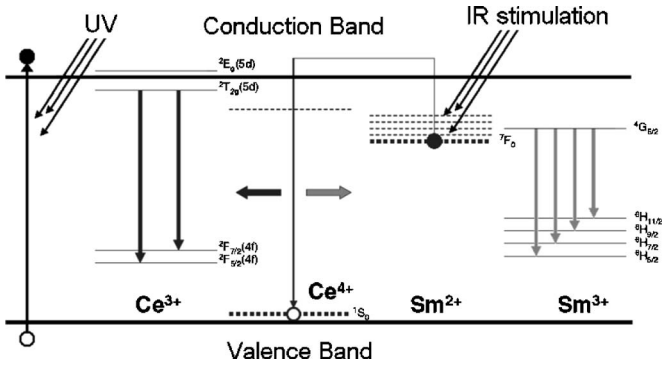

FIG. 2. OSL mechanisms as reviewed in Ref. 18 following the Keller model. During exposure to UV light, electrons and holes are produced in the conduction and in the valence band of the SrS. Part of this energy is stored in metastable levels modifying the valence states of the two activators, initially in the trivalent (+3) state: Ce^{3+} become Ce^{4+}, while Sm^{3+} become Sm^{2+} acting as an electron trap. Under IR stimulation, the trapped electron is ejected via the conduction band, then is recombined with Ce^{4+} becoming an excited state of Ce^{3+}. The return to the ground state of Ce^{3+} gives the observed characteristic Ce^{3+} emissions. In the same way, at much lower rate, electrons can directly recombine within the Sm^{3+} levels, emitting a series of weak characteristic lines.

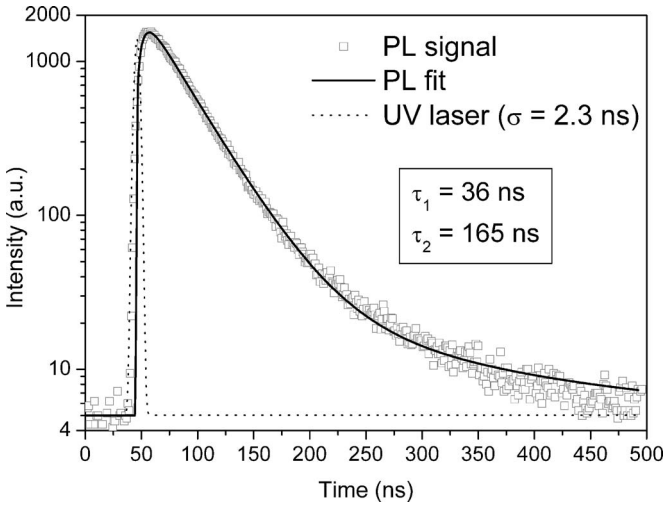

FIG. 3. Photoluminescent (PL) decay curve from the SrS:Ce,Sm phosphor following a 260 nm excitation over a 500 ns time base. The curve has been recorded in the spectral range 490±30 nm corresponding to the main Ce^{3+} emission. The dotted curve represents the temporal behavior of the 260 nm, 2 ps laser pulse as recorded by the streak scope.

536 nm are due to transitions from the $5d$ state to the $4f$ ($^2F_{5/2}$, $^2F_{7/2}$) state of the Ce^{3+} activator ion. Since the $4f$ state of the activator is shielded from the influence of the surrounding, the crystal field of the host material causes only a small perturbation to the $4f$ state. The energy separation between the $^2F_{5/2}$, and the $^2F_{7/2}$ levels of the $4f$ state in sulfides remains, therefore, approximately the same as in the free ion generating these two typical emission bands. On the other hand, the $5d$ state is sensitive to the crystal field and strongly couples with the SrS lattice vibrations, as shown in Fig. 2.

The long-lasting weak emissions rather arise from the transitions $4f$ ($^4G_{5/2}$)$\rightarrow 4f$ ($^6H_{5/2}$, $^6H_{7/2}$) of the Sm^{3+} coactivator ion (see the right-hand side of Fig. 2). Following Ref. 20, this long-lived luminescence is due to the particular local environment of the Sm^{3+} ion, formed by charge compensation, in the lattice position of the SrS host. This characteristic luminescence is the evidence that Sm^{3+} ion induces defects in the crystal lattice that are thought to be involved in electron trapping and, in turn, responsible for the storability proprieties of this particular SrS phosphor.[21] The characteristic PL spectrum of the Sm^{3+} ion extends above 600 nm with other characteristic lines[18] that have not been measured in this study.

B. Photoluminescence measurements

In order to measure the characteristic times of the fast Ce^{3+} PL emissions, Fig. 3 shows the decay curve of the luminescence signal following 2 ps UV-laser excitation recorded over a 500 ns time window. Although it has been observed that all wavelengths of the fast-luminescent spectrum have similar time behaviors, the quantitative analysis has been done by integrating only the PL signal corresponding to the main Ce^{3+} emission (spectroscopy windows centered at λ_c=490±30 nm). The Ce^{3+} light-emitting mechanism can be summarized with the following classical first-order reaction scheme for the production of luminescence:[22]

$$Ce^{3+} + h\nu_1 \xrightarrow{\text{fast}} Ce^{3+,*} \xrightarrow{\tau_i} Ce^{3+} + h\nu_2, \quad (1)$$

where ν_1 and ν_2 are the frequencies of the exciting and emitted photons, respectively, when the excitation rate, indicated by "fast" in Eq. (1), is higher than the emission rates (τ_i). Following this scheme, the luminescence rise and decay curves can be fitted with the sum of exponential functions. For all data presented in this work, the fitting functions have been convoluted with the whole apparatus response that is a Gaussian function of a given standard deviation (see dotted lines in the presented figures).

As shown in Fig. 3, upon excitation at λ=260 nm, the initial stage of the luminescence follows a pure exponential decay characterized by a time constant (τ_1) of 36±1 ns. This value is typical for the lifetime of the Ce^{3+} $5d\rightarrow 4f$ transitions, as measured in different scintillating materials.[23–25] Bibliographic values for τ_1 in Ce-doped inorganic materials lie in the 20–30 ns range. Although the luminescence is always emitted by transitions between electronic levels of the activator ion, the variations in τ_1 for different scintillating materials can be explained with the strong coupling of the Ce^{3+} $5d$ state with the crystal field of the host compound, as already mentioned in the previous section. Even if the decay curve quickly reaches the noise level, the exponential PL decay also presents a slower exponential tail that can be characterized with a second time constant (τ_2) of 165±20 ns.

In order to measure the rise time of the Ce^{3+} photoluminescence, a second image has been taken on a 50 ns time scale, as shown in Fig. 5. From the picture, it is clear that the luminescence rises with a finite time after the excitation by the sharp laser pulse (dotted Gaussian shape in Fig. 5 with full width at half maximum of 0.42 ns). Fitting this new data set with a double-exponential curve, using the previously measured decay time (τ_1) as parameter, is then possible to obtain a luminescent rise time constant ($\tau_{r,\mathrm{PL}}$) of 2.5±0.5 ns. This measurement shows that the energy transfers from the excitons to Ce^{3+} ions are fast and efficient.

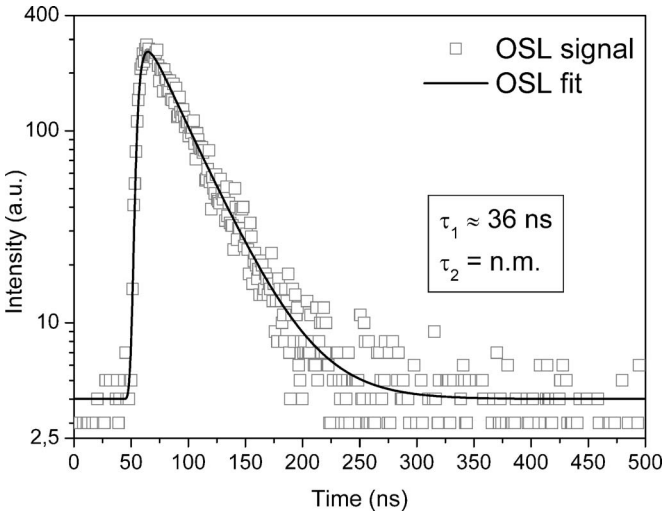

FIG. 4. Optically stimulated luminescence (OSL) decay curve from the SrS:Ce,Sm phosphor following an 805 nm excitation over a 500 ns time base. The curve has been recorded in the spectral range 490±30 nm corresponding to the main Ce^{3+} emission. The trapped charge was previously generated in the material by exposing it for 5 min to a constant flux of 254 nm UV light. The fist stage of the exponential luminescent decay is here again well fitted with a lifetime (τ_1) of 36 ns. The tail of the OSL is not measurable (n.m.) here since the weak OSL emission falls quickly down to the noise level.

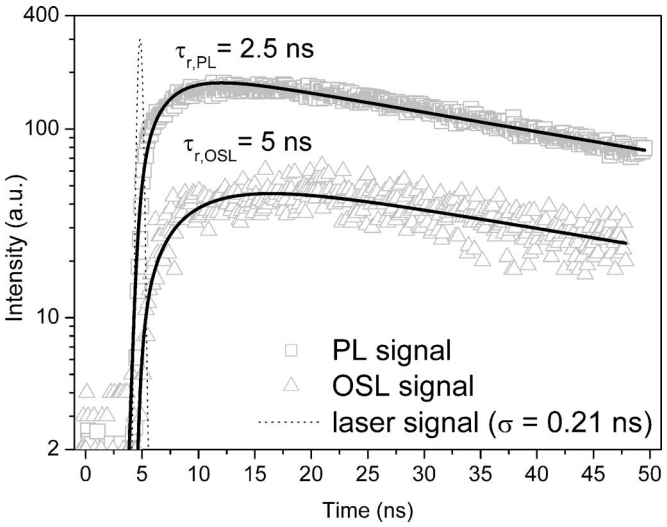

FIG. 5. PL and OSL rise/decay curves from the SrS:Ce,Sm phosphor following 260 and 805 nm laser excitations over a 50 ns time base. The dotted curve represents the temporal behavior of the 2 ps laser pulses as recorded by the streak scope.

C. Optically stimulated luminescence measurements

The measurements presented in the previous section have been repeated in the OSL regime stimulating with IR-laser pulses the charges stored in the SrS:Ce,Sm phosphor by a previous UV-light exposure. As shown in Fig. 4, OSL measurements over a 500 ns scale revealed the same emission spectrum with an equal characteristic lifetime τ_1 to that for the luminescence decay obtained in the PL experiment (Fig. 3). Due to the low intensity of the recorded OSL signal, it was not possible, in this case, the measurement of a second characteristic lifetime. Nevertheless, this result confirms the predominant role of the activator ion in the fast-luminescent emission process in both OSL and PL phenomena.

Figure 5 also shows the OSL time-resolved measurement over a 50 ns time scale. The best fit of the OSL gives a rise time constant ($\tau_{r,\mathrm{OSL}}$) of 5.0±1 ns. The error affecting the measurement is here increased due to the lower statistic of the OSL signal as visible looking at the scattering of the points in the luminescent curve decay. This is due to the experimental difficulty in measuring a luminescent signal that quickly depletes over time in the OSL experiment.

The luminescence rise time in OSL turns out to be 5.0±1 ns, that is, 2.5 ns longer with respect the one measured in the PL experiments. The origin of this delay in the OSL signal buildup can be here interpreted by using the existing OSL models. Under IR stimulation, the trapped electrons are ejected from the Sm^{3+} centers and raised to the conduction band of the host material, as shown in Fig. 2. The following recombination of the electrons with the Ce^{3+} activator ion brings it to an excited state. The final return to its ground state gives the observed characteristic emission measured in the OSL experiments. This model was first proposed by Keller *et al.*[26] in 1958. Nowadays, the real nature of the trapping Sm^{+3} states is still under discussion,[21] and some authors also believe that electron transfer does not involve the conduction band[4] but that it can take place directly within the defect complexes formed by the rare earths with the sulfide ions.[27]

The experimental data presented here do not bring any element in favor of or against the different OSL microscopic models for the SrS:Ce,Sm. However, it is important to remember that the charge detrapping step is the key element that makes the difference between the OSL and the PL experiments. In fact, the PL signal is generated by direct excitation of the Ce^{3+} activator ion following the absorption of the energetic UV-laser photons (4.8 eV) and without involving the charge trapped in the coactivator states (Sm^{+3}).

The difference in the rise time of the two luminescent curves measured in this work can therefore be considered as a valuable indication of the rapidity of the charge conversion of the investigated SrS:Ce,Sm material.

IV. DISCUSSION AND CONCLUSION

Time-resolved measurements have been carried out on the SrS:Ce,Sm OSL material synthetized at the University Montpellier II in France. The lifetime of the luminescent decay (τ_1), in both OSL and PL experiments, has been found to be equal to 36±1 ns. This value, determined by the activator ion species, agrees with the typical luminescence lifetime of Ce-activated fast inorganic scintillating crystals and extends a previous work of Gasiot *et al.*[5] on doubly activated SrS phosphors. A slower lifetime tail (≈165 ns) in the PL decay has also been measured. A detailed discussion of this second luminescent stage has not been possible since the luminescent signal fell quickly down to the noise level.

The measured decay time shows that the investigated material is not adapted for the detection of very fast phenomena ($\tau \approx 25$ ns) in harsh radiation fields, as in the case of the next generation of HEP experiments like the ones at the CERN LHC. For this latter application, organic scintillators

and chemical vapor deposition diamond detectors remain still the best compromise joining a faster response time (about one order of magnitude lower than the one measured here for our SrS phosphor) and good radiation hardness.

On the other hand, this work provides a direct measurement on the charge conversion time in the SrS:Ce,Sm by comparing the results of the PL and OSL measurements. The characteristic time for the charge detrapping has been measured here to be 2.5 ± 1 ns. This time is of importance, considering the possibility to use this stimulable phosphor in optical memory applications. Details on these applications are available in Refs. 6 and 7. Although the following radiative transition takes several tens of nanoseconds, the possibility to perform the "read" process of the stored information (e.g., trapped electrons) on a nanosecond time scale is an interesting prospect. Moreover, it should be pointed out that this detrapping time might be strongly affected by the degree of filling of the trapping states and by the power of the stimulating IR-laser light. These possible dependences suggest further investigations on this phosphor with repeated time-resolved experiments.

[1]K. Chakrabarti, V. K. Mathur, J. F. Rhodes, and R. J. Abbundi, J. Appl. Phys. **64**, 1363 (1988).
[2]K. Chakrabarti, V. K. Mathur, L. A. Thomas, and R. J. Abbundi, J. Appl. Phys. **65**, 2021 (1989).
[3]J. Weiwei, X. Zheng, Z. Fujun, Z. Xiyan, and W. Liwei, J. Mater. Process. Technol. **184**, 93 (2001).
[4]K. Chakrabarti, V. K. Mathur, and R. J. Abbundi, Phys. Rev. B **39**, 10406 (1989).
[5]J. Gasiot, P. Bräunlich, and J. P. Fillard, J. Appl. Phys. **53**, 5200 (1982).
[6]H. Nanto, Y. Douguchi, J. Nishishita, M. Kadota, N. Kashiwagi, T. Shinkawa, and S. Nasu, Jpn. J. Appl. Phys., Part 1 **36**, 421 (1997).
[7]V. G. Kravets, Opt. Mater. (Amsterdam, Neth.) **16**, 369 (2001).
[8]O. Missous, F. Loup, J. Fesquet, H. Prevost, J. Gasiot, J. P. Sanchez, and C. A. Dos Santos, Eur. J. Solid State Inorg. Chem. **28**, 163 (1991).
[9]K. Idri, L. Santoro, E. Charpiot, J. Herault, A. Costa, N. Aillères, R. Delard, J. R. Vaillé, J. Fesquet, and L. Dusseau, IEEE Trans. Nucl. Sci. **51**, 3638 (2004).
[10]D. Plattard, G. Ranchoux, L. Dusseau, G. Polge, J.-R. Vaillé, J. Gasiot, J. Fesquet, R. Ecoffet, and N. Iborra-Brassart, IEEE Trans. Nucl. Sci. **49**, 1322 (2002).
[11]F. Ravotti, M. Glaser, M. Moll, K. Idri, J.-R. Vaillé, H. Prevost, and L. Dusseau, IEEE Trans. Nucl. Sci. **51**, 3642 (2004).
[12]A. Fernandez Fernandez, B. Brichard, F. Berghmans, S. O'Keeffe, C. Fitzpatrick, E. Lewis, J.-R. Vaillé, L. Dusseau, D. A. Jackson, F. Ravotti, M. Glaser, and H. El-Rabii, Fusion Eng. Des. (in press).
[13]A. Gorišek, V. Cindro, I. Dolenc, H. Frais-Kölbl, E. Griesmayer, H. Kagan, S. Korpar, G. Kramberger, I. Mandić, M. Meyer, M. Mikuž, H. Pernegger, S. Smith, W. Trischuk, P. Weilhammer, and M. Zavrtanik, Nucl. Instrum. Methods Phys. Res. A **572**, 67 (2007).
[14]M. Gallart, Ph.D. thesis, University Montpellier II, 2001.
[15]J. Gasiot, P. Bräunlich, and J. P. Fillard, Appl. Phys. Lett. **40**, 376 (1982).
[16]W. Fan, Y. Wang, X. Hou, L. Du, W. Zhao, B. Yang, and L. Niu, J. Appl. Phys. **85**, 451 (1999).
[17]P. Bräunlich, D. Schäfer, and A. Scharmann, Proceedings of the First Conference on Luminescence Dosimetry, Standford, CA, 1967, p. 57; Report No. USAEC-650637, 1965.
[18]D. Lapraz, H. Prévost, K. Idri, G. Angellier, and L. Dusseau, Phys. Status Solidi A **203**, 3793 (2006).
[19]V. Singh, M. Tiwari, T. K. Gundu Rao, and S. J. Dhoble, Bull. Mater. Sci. **28**, 31 (2005).
[20]J. Wu, D. Newman, and I. V. F. Viney, J. Phys. D **35**, 968 (2002).
[21]H. Zhi-Yi, W. Yong-Sheng, S. Li, and X. Xu-Rong, J. Phys.: Condens. Matter **13**, 3665 (2001).
[22]B. J. Selby, T. I. Quickenden, and C. G. Freeman, Kinetics and Catalysis **44**, 5 (2003).
[23]E. Radzhabov and T. Kurobori, Radiat. Meas. **38**, 523 (2004).
[24]N. J. M. Le Masson, A. J. J. Bos, and C. W. E. Van Eijk, Radiat. Meas. **33**, 693 (2001).
[25]V. P. Dotsenko, I. V. Berezovskaya, N. P. Efryushina, E. V. Shabanov, and A. S. Voloshinovskii, Phys. Status Solidi A **203**, 892 (2006).
[26]S. P. Keller, J. E. Mapes, and G. Cheroff, Phys. Rev. **108**, 663 (1958).
[27]M. I. Danilkin, M. P. Kerikmäe, S. O. Klimonsky, V. D. Kuznetsov, E. F. Makarov, Ju. V. Permyakov, A. E. Primenko, and V. O. Seeman, Nucl. Instrum. Methods Phys. Res. A **537**, 89 (2005).